13èmes Journées de l'Hydrodynamique
21 - 23 novembre 2012
Laboratoire d'Hydraulique Saint-Venant
Ile des Impressionnistes,
Chatou (78), France

DETERMINISTIC PREDICTION OF OCEAN WAVES BASED ON X-BAND RADAR MEASUREMENTS

PREVISION DETERMINISTE DE HOULE A PARTIR DE MESURES PAR RADAR A BANDE X

E. BLONDEL-COUPRIE[*], P. NAAIJEN[*]

[*] Dept. Ship Hydromechanics and Structures, Faculty 3ME
Delft University of Technology, Delft, The Netherlands
E.H.M.Blondel-couprie@tudelft.nl

Summary

The final goal of the study is to develop a real-time (60s to 120s ahead) onboard decision support system for offshore operations involving a ship moving in waves, based on a deterministic prediction of its wave-induced motions. Since the motions calculation is completely dependant on the sea state at the ship location, this paper focus on the development of a deterministic prediction model for the sea surface elevation.

The presented work aims to assess the feasibility of initializing such a deterministic prediction model based on spatio-temporal measurements of the ocean surface made by means of an X-Band Radar, classically used for navigation purpose. The main questions raised are: What exactly is the output of an X-Band Radar analysis system? Can X-Band Radar measurements be directly used as input for a wave propagation model? More precisely, focus is on the 3DFFT (3D Fourier Transform) analysis which is the basis of such Radars image processing systems. It is investigated whether the wave components obtained by this 3DFFT analysis can be used to derive a proper initialization for a wave propagation model, enabling further deterministic prediction of the sea state.

Résumé

Ce travail de recherche a pour objectif final le développement d'un outil d'aide à la décision en temps réel (60 à 120s en avance) pour les opérations offshore requérant une connaissance précise des mouvements d'un navire soumis à la houle, basé sur une prévision déterministe de ces mouvements. Le calcul des mouvements du navire étant complètement dépendant de la connaissance de l'état de mer en présence, les résultats présentés dans cet article se rapportent uniquement à la prévision déterministe de la houle.

L'étude présentée a pour objectif de déterminer si un tel modèle de prévision déterministe peut être initialisé par des données de houle fournies un Radar à bande X, classiquement utilisé pour la navigation. Les principales questions posées sont : Quelles sont exactement les données de houle fournies par un système d'analyse de données Radar à bande X ? Peuvent-elles être introduites telle quelles dans un modèle de propagation de houle ? Dans cet article, nous nous sommes plus particulièrement intéressés à l'analyse par Transformée de Fourier 3D (3DFFT) sur laquelle les systèmes d'analyse d'image Radar à Bande X reposent. Il s'agit de déterminer si les composantes de houle obtenues par le biais de l'analyse par 3DFFT peuvent permettre de trouver une condition initiale au modèle de propagation de houle, afin d'obtenir une prévision déterministe de l'état de mer.

I. INTRODUCTION

Until now, existing decision systems commonly used for offshore applications – such as decommissioning operations, man transfer on plate-forms, installation or maintenance operations, helicopter landing, etc…– rely on statistical predictions. Based on the knowledge of the sea spectrum, the probability that one or more relevant parameters exceed the operability criteria is evaluated and the operation allowed or cancelled. To insure the safety of these operations, strict empirical conditions are usually imposed. The counterpart is that these restrictions are limiting the operations in terms of logistics and planning.

Some attempts are made to develop new decision systems based on a better understanding of the physics involved in ship motions in waves, instead of empirical data. However, such systems still only provide a more precise *indication on the operability*. They do not provide a way to *improve the operability*. Moreover, since these decision support systems rely on statistical quantities describing the sea state (which are averaged over 2 or 3 hours), they do not consider the waves in real-time. Real-time decision systems which advise about the optimal timing for operations in a short-term constraint do not currently exist.

A way to improve the operability of offshore operations involving a ship moving in waves is to provide a *deterministic prediction* (time traces) of these wave-induced ship motions: knowing in real-time the ship motions will enable to determine a short-time period in which the ship motions are acceptable. This not only improves the workability of the operation, but also the safety of the procedure since the operator is able to avoid risky situations.

Of course, the calculation of the wave-induced ship motions is totally subjected to the encountered waves. Therefore, the critical issue is the accurate prediction of the sea surface at the ship location. The development of a real-time deterministic wave prediction model is a very challenging task because of the complexity of the physics involved in the wave process, and of the constraint on the limited calculation times. Moreover, the accurate prediction of a given sea state is subjected to an accurate measurement of the incoming waves.

But the development of efficient computing technologies and remote wave sensing devices ([2], [10], [11]) makes it feasible to consider deterministic predictions of wave and induced ship motions as an alternative to statistical predictions. With the increasing demand on accurate wave data from the offshore industry, the topic has thus begun to attract significant attention ([4], [7], [8], [10], [12], [13], [16], [18], [20]). In this case, the aim is to use an X-Band Radar as wave sensor. As a matter of fact, X-Band Radars are already available on most of the offshore vessels since they are used to help the navigation by detecting surrounding obstacles (ships, platforms …).

Starting with the OWME project in 2008 ([16], [15]), TU Delft has been very active in this research field. Since 2012, the SHS research group is involved in 2 new research projects on the topic (SBIR: "Online motion prediction of navy vessels in heavy weather" and PROMISED Operation: "PRediction Of wave induced Motions and forces In Ship, offshore and Dredging Operations"). The third paragraph of this paper reports on the progress achieved within these research projects. Focus is on the initialization of a wave model with wave data provided by X-Band Radar images processing (IP) systems such as WaMoS (see [11]).

Since a few decades, X-Band Radars have been used to derive wave spectra, current speed or water depth. The general IP method for deriving these quantities has been validated extensively, starting with the paper by Young et al [19]. However, the use of X-Band Radars for deterministic wave sensing is quite new. Very few studies have been conduced to assess the accuracy of time series of the ocean surface obtained from the X-Band Radar IP systems. Lately an experimental campaign has been conduced to validate WaMoS wave measurements to Lidar measurements (plane-mounted). However, the results have not been published yet.

The main difficulty related to wave measurements by means of an X-Band Radar is that there is no direct measurement of the wave elevation. The sensor captures backscattered intensities of the reflected Radar magnetic waves on the ocean surface. These *intensity images* must thus be converted into *wave images*.

To do so, X-Band Radar IP systems commonly rely on a 3D Fourier analysis (in both space and time domains) of those intensity images. The 3DFFT analysis serves 3 goals: i) remove the directional ambiguity on the main propagation of the waves, ii) filter the background noise from wave components by using the linear dispersion relation (LDR) as a filter, iii) enable the application of a Modulation Transfer Function (MTF) in the frequency domain to convert the intensity components into wave components.

The question addressed in the present study is the possibility of finding a proper initialization for a wave propagation model from the results of a 3DFFT applied to observations. In order to simplify the problem and only focus on the 3DFFT issues, the Radar IP procedure is mimicked by using "perfect" synthetic wave images. Thereby, inaccuracies due to measurement noise, and the use of an empirical MTF to convert intensity components into wave components, are discarded.

Synthetic waves are generated by means of a linear wave model in a given domain in space and time. Within this domain, only a restricted area in space and time is considered as the *observation zone*, on which the 3DFFT analysis is applied. This observation zone, as well as its discretization is time and space, is comparable to the one of a wave Radar.

We then present a specific approach for manipulating the Fourier components obtained by applying a 3DFFT to wave observations. This approach consists in deriving, from the 3DFFT results, underlying linear wave components of the wave field, considering the linear dispersion relation as a filter. The efficiency of the method is investigated in terms of *reconstruction* (the surface elevation is estimated in the *observation zone*) and *prediction* (the surface elevation is estimated at further times). It is shown that the method allows for accurate predictions of the wave field.

II. 3DFFT ANALYSIS OF WAVE IMAGES AND DETERMINISTIC PREDICTION

II.1 3DFFT analysis in X-Band Radar image processing systems

X-Band Radars are mounted on most of the current vessels to detect other ships in the surroundings and avoid possible collisions. To do so, the reflections on the ocean surface of the Radar electromagnetic waves are filtered out since they hamper the detection of the ships nearby. However, these "spurious" reflections contain significant information about the wave field that the ship is encountering.

Since a few decades, this information has been used to estimate averaged directional wave spectra, water depth, or current speed. The analysis via a 3DFFT of X-Band Radar measurements to retrieve wave spectra has been validated extensively in the literature. However, no study has been reported yet on the validation of this approach for deterministic purpose (ie retrieving time series of the surface elevation instead of averaged statistical properties).

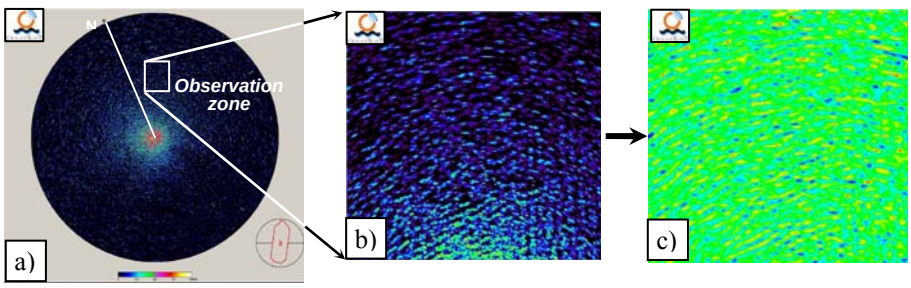

Figure 1 : Conversion of intensity images measured by an X-Band Radar to wave images.

Retrieving wave elevations from X-Band Radar measurements is not trivial. The main issue to convert what is actually measured by the Radar, which are intensity images of the

reflected electromagnetic waves, into wave images (see Figure 1). Many features make it a difficult task: the Radar intensity power decay with the range, the Radar polar resolution (the furthest from the antenna, the less refined discretization), the rotation of the antenna (all the points of a Radar image are not measured at the same time), the shadowing effect which increases with the distance to the antenna (a wave is partly hidden from the Radar beam by the previous wave in the direction of the antenna), the background noise, to name a few.

The key points of the analysis which is commonly used in X-Band Radar IP to convert intensity images to wave images are given in Figure 2. More details can be found in [17]. As can been seen on the figure, the procedure starts with a 3DFFT; all the following steps of the analysis are then conducted in the Fourier domain. The 3DFFT thus plays a fundamental role in the process.

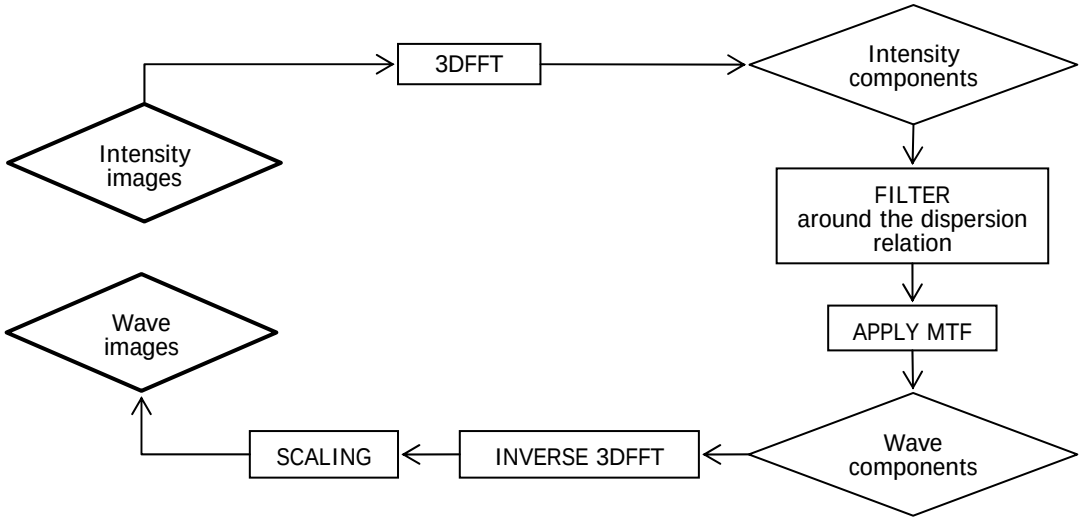

Figure 2 : Principle scheme of an X-Band Radar image analysis system.

A stack of intensity images is first selected from the Radar records in specific area in space and time referred to as the *observation zone* (see Figure 1). A 3DFFT is then applied to this series of images to obtain directional intensity frequency components (ie having each a two dimensional wave number **k** and a frequency ω). This enables:

- To determine the main propagation direction of the waves (are the waves travelling forward or backward?); this cannot be achieved by considering only one image and applying a 2DFFT on this image since a 2DFFT returns symmetric complex amplitudes.
- The distinction between background noise and real wave patterns: considering that noise is a chaotic process and does not propagate the same way waves do, it can be distinguished from the ocean waves by applying a bandpass filter around the LDR.
- The transfer from intensity components into wave components by applying an MTF, which is defined in the Fourier domain, to the filtered intensity components. This step is critical for the Radar image analysis. As a matter of fact, the MTF is supposed to account for all the mechanisms (tilt & hydrodynamic modulations, shadowing) which have to be considered when converting intensity spectra to wave spectra. There is currently no real analytic expression for each of these mechanisms. They are indeed very chaotic and strongly dependent on local weather conditions such as wind. The MTF is thus usually derived from experiments.

An inverse 3DFFT is finally applied to the obtained wave components to obtain the surface elevation. Note that, because the wave amplitudes are not calibrated (they reflect the intensity of the backscatter measured by the Radar), the wave elevation has to be scaled.

It is important to point out that the output of this analysis is a wave field which is periodic in both time and space domains, due to the periodicity of the 3DFFT. This is quite unrealistic since real ocean waves are not periodic. Thus, it is hardly possible to determine a realistic and accurate prediction of the wave field using only 3D Fourier representation.

II.2 Problem addressed

The aim of this study is not to address the topic of the MTF although it is a crucial part in the Radar IP as mentioned above. Our purpose is to gain more understanding in the general Radar IP approach, and particularly on the use of 3DFFT analysis and its implications for deterministic prediction calculations. Discarding all the considerations associated to real Radar measurements (noise, MTF), and considering perfect measurements of the sea surface elevation, the questions are:

- What is the result of a 3DFFT applied to a stack of wave images?
- Can the wave components obtained by the 3DFFT be used to derive a proper initialization for a wave propagation model?

Let us consider images of size $L_x \times L_y$ of the wave elevation η(**x**,t) recorded during a period T (see Figure 4). The observation zone is of size $N_x \times N_y \times N_t$, where N_x and N_y are the number of discretization points considered in x and y directions, while N_t is the number of wave maps recorded. Applying a 3DFFT to this stack of wave images yields decomposition (1) of the surface elevation into $N_x \times N_y \times N_t$ directional wave components. Each Fourier component has a complex amplitude A_{ijn}, a wave number $\mathbf{k}_{ij} = (k_{x_i}, k_{y_j})$ defined by (2) and a frequency ω_n defined by (3). Note that the 3DFFT is symmetric in a way that the complex 3D amplitudes verify (4).

$$\eta(\mathbf{x},t) = \sum_{i=1}^{N_x/2+1} \sum_{j=1}^{N_y} \left\{ \sum_{n=1}^{N_t/2+1} \underline{A_{ijn}} \exp[i\,\omega_n t] + \sum_{n=N_t/2+2}^{N_t} A_{ijn} \exp[-i\,\omega_n t] \right\} \exp[i\,\mathbf{k}_{ij} \cdot \mathbf{x}] + \text{conj} \tag{1}$$

where

$$\begin{cases} k_{x_i} = \dfrac{2\pi(i-1)}{L_x} & , \; i \in \left[1, \dfrac{N_x}{2}+1\right] \\ k_{x_i} = -k_{x_{N_x-i+2}} & , \; i \in \left[\dfrac{N_x}{2}+2, N_x\right] \end{cases} \quad \text{and} \quad \begin{cases} k_{y_j} = \dfrac{2\pi(j-1)}{L_y} & , \; j \in \left[1, \dfrac{N_y}{2}+1\right] \\ k_{y_j} = -k_{y_{N_y-j+2}} & , \; j \in \left[\dfrac{N_y}{2}+2, N_x\right] \end{cases} \tag{2}$$

$$\begin{cases} \omega_n = \dfrac{2\pi(n-1)}{T} & , \; n \in \left[1, \dfrac{N_t}{2}+1\right] \\ -\omega_n = -\omega_{N_t-n+2} & , \; n \in \left[\dfrac{N_t}{2}+2, N_t\right] \end{cases} \tag{3}$$

$$\underline{A_{ijn}} = CONJ\left(\underline{A_{N_x-i+2,N_y-j+2,N_t-n+2}}\right) \;, \quad i \in \left[\frac{N_x}{2}+2, N_x\right] , \; j \in \left[\frac{N_y}{2}+2, N_y\right] , \; n \in \left[\frac{N_t}{2}+2, N_t\right] \tag{4}$$

Since the observation domain is finite in both space and time domains, only a limited number of Fourier components, associated to the $N_x \times N_y$ wave numbers $\mathbf{k}_{ij}$ and the N_t frequencies ω_n, are used to describe the measured surface elevation which certainly contains an infinite number of wave components. Besides, even if we would only consider the wave components present in the measured wave field which contain significative energy, there is very little chance that their frequencies and wave numbers match the ones of the Fourier analysis.

Thus spectral leakage occurs in both time and space domains, ie the energy initially present in the wave field at a given frequency and wave number is transferred to all the frequencies and wave numbers of the Fourier analysis. More precisely, the energy carried by a component of the wave field is mostly transferred to the Fourier component whose frequency/wave number are the closest to the ones of the original wave component, but some energy is also spread on the other Fourier frequencies and wave numbers.

Spectral leakage occurs regardless of the order of non-linearity of the wave field, as illustrated on Figure 3. This figure shows the results of a 3DFFT applied to a stack of synthetic linear wave images.

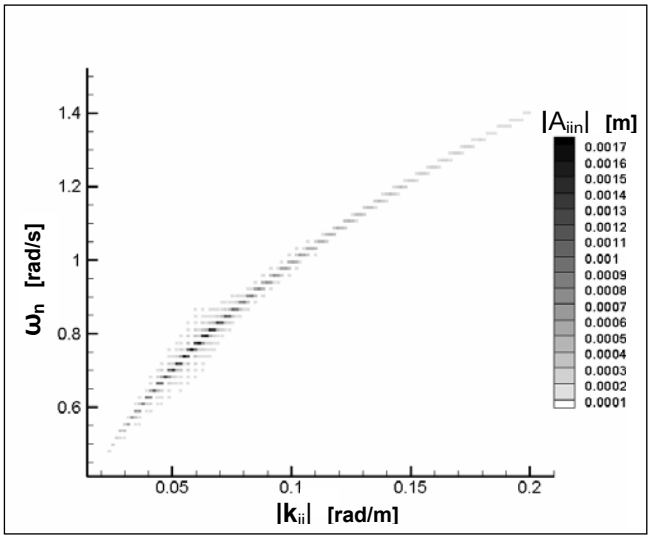

Figure 3 : Illustration of spectral leakage associated to the application of a 3DFFT to a stack of wave images. In this case, synthetic waves have been generated with a linear model.

Spectral leakage due to 3DFFT analysis is not an issue for deterministic wave reconstruction when considering perfect wave data (no noise), ie when the aim is to obtain, from the Fourier components, an estimation of the measured wave field in the same observation zone as the one on which the 3DFFT was applied. The wave field can simply reconstructed by an inverse 3DFFT applied to the Fourier components.

Spectral leakage becomes a problem when the objective is to obtain an estimate of propagated wave field, ie for deterministic prediction purpose. The question is: how propagate the wave components resulting from spectral leakage? In fact, these wave components carry energy of the original wave field components, but not at the same velocity. Besides, these components have wave numbers and frequencies which do not match the LDR (given in (5)). But any wave propagation model, being linear or non-linear, requires as input wave components whose frequencies and wave numbers exactly match the LDR.

$$\omega = \sqrt{g|\mathbf{k}|\tan(|\mathbf{k}|h)} \tag{5}$$

This suggests that the wave components provided by X-Band Radar IP, discarding the issues associated to measurement noise or MTF related IP difficulties, cannot be directly used as initialization for a wave propagation model. The problem addressed in this paper is therefore to assess the feasibility of finding a proper initialization for a propagation model, from the result of a 3DFFT analysis applied to a stack of images.

To simplify the study, we consider images of synthetic waves generated with a linear model. Inaccuracies due to non-linearities, measurement noise or empirical MTF are thereby eliminated. The observation domain and its resolution in time and space are equivalent to the ones of a wave Radar.

Since the objective is to derive from the 3DFFT result a set of linear wave components which can be used to initialize a wave propagation model, we consider the LDR as a "filter". Various attempts are investigated to "manipulate" the 3D Fourier wave components in order to retrieve the underlying linear wave components of the wave field. Their accuracy in terms of wave field reconstruction and prediction is investigated.

III. RECONSTRUCTION AND PREDICTION OF SYNTHETIC WAVE DATA WITH DIFFERENT APPROACHES BASED ON 3DFFT ANALYSIS

III.1 Synthetic linear wave images

$$\eta(\mathbf{x},t) = \sum_{i=1}^{N_1}\sum_{j=1}^{N_2} \widetilde{A}_{ij} \cos\left[-\widetilde{\omega}_{ij}t + \widetilde{k}_{x_i}x + \widetilde{k}_{y_j}y + \widetilde{\varphi}_{ij}\right]$$

where

$$\begin{cases} \widetilde{A}_{ij} = \sqrt{2\dfrac{g^2}{\widetilde{\omega}_{ij}^3} E(\widetilde{\omega}_{ij},\widetilde{\theta}_{ij})\Delta\widetilde{k}_{x_i}\Delta\widetilde{k}_{y_j}} \quad ; \quad \widetilde{\varphi}_{ij} = U[0,2\pi] \\ \widetilde{\theta}_{ij} = \arctan\left(\widetilde{k}_{y_j} \Big/ \widetilde{k}_{x_i}\right) \\ \widetilde{\omega}_{ij} = \sqrt{g\left|\widetilde{\mathbf{k}}_{ij}\right| \tanh\left(h\left|\widetilde{\mathbf{k}}_{ij}\right|\right)} \end{cases} \tag{6}$$

The so-called "Single summation method" is applied to generate synthetic short-crested waves from a linear superposition of wave components (see (6)). We assume that the wave amplitude $\widetilde{A}_{ij}$ of each component can be found by a (discretized) directional energy spectrum $E(\widetilde{\omega}_{ij},\widetilde{\theta}_{ij})$. In our applications, we consider a directional JONSWAP spectrum based on a $\cos^2$ analytic directional spreading function. The phase angles are uniformly distributed in $[0,2\pi]$ via the uniform distribution function U.

To ensure that the wave numbers and/or the frequencies used for the generation do not match the ones used in the Fourier analysis, the wave fields are generated from non-equally spaced wave numbers $\widetilde{\mathbf{k}}_{ij}$. In expression (6), the steps $\Delta\widetilde{k}_{x_i}$ and $\Delta\widetilde{k}_{y_j}$ are therefore non constant.

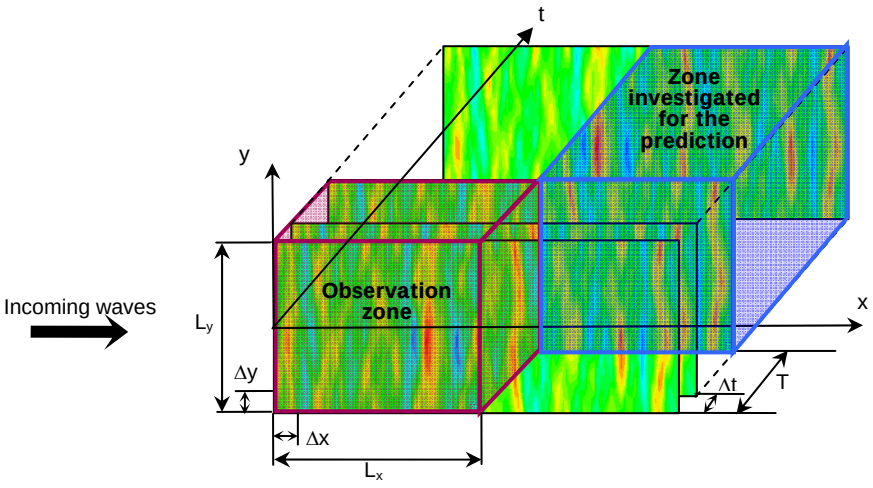

Figure 4 : Generation of synthetic wave data.
Observation zone and zone investigated for the prediction calculations.

192 images of the synthetic ocean surface are generated. The images are discretized by 256×128 points which are equidistant from 7.5m. The time step between two consecutive images Δt is chosen equal to 1s. The considered wave conditions are classical North-sea conditions: $\{H_s$=1m, T_p=8s, θ_0=0°, θ_s=30°$\}$, where H_s is the significative wave height, T_p the peak period, θ_0 the main propagation direction and θ_s the angular spreading. We point out that the significative wave height is not relevant here since we only consider linear waves.

The observation zone is selected from the created wave images at the N_t=64 first time steps (ie measurement period of T=64s). It has a size of $N_x \times N_y$=128×128 points in space which corresponds to an area of $L_x \times L_y \approx$1km². This is depicted on Figure 4.

III.2 A new approach for analysing the results of a 3DFFT applied to wave observations

As mentioned in section II.2, the energy initially carried by a given component of the measured wave field is spread on all the frequencies/wave numbers of the 3D Fourier analysis due to spectral leakage in both space and time domains. The issue is to be able to represent as accurately as possible the synthetic wave field by linear wave components obtained from the 3D Fourier components. The aim is to find a representation of the observed wave field as described in (7) from the 3DFFT result given in (1).

$$\eta(\mathbf{x},t) = \sum_{i=1}^{N_x/2+1} \sum_{j=1}^{N_y} \underline{A_{ij}^f} \exp\left[-i\,\omega_{ij}^f t\right] \exp\left[i\,\mathbf{k}_{ij}^f \cdot \mathbf{x}\right] + \text{conj} \tag{7}$$

This section describes different ways of manipulating the 3D Fourier components by using the LDR as a filter. The proposed filters differ by:

- The choice of the couples frequencies/wave numbers $\mathbf{k}_{ij}^f / \omega_{ij}^f$ satisfying the linear dispersion relation,
- The choice of the associated complex amplitudes $\underline{A_{ij}^f}$.

Regarding the first point, an option consists in considering that the underlying linear wave components have wave numbers equal to the Fourier wave numbers $\mathbf{k}_{ij}$ (given in (2)). Their frequencies are then derived from these wave numbers using the LDR. (Thereby, instead of n Fourier frequencies associated to one Fourier wave number, only the frequency matching the LDR is considered.) This option is referred to as Option 1 and is described in (8).

The other option is to consider the Fourier frequencies ω_n (given in (3)) and recalculate the wave numbers according to the LDR. This option is referred to as Option 2 and is described in (9). In this case, the propagation direction associated to a given wave component remains equal to the propagation direction associated to the initial Fourier wave number at this Fourier frequency, as written in (10).

The first option is much more attractive that the second one since it enables to estimate the surface elevation by an inverse 2DFFT in space of the filtered time dependent amplitudes. In case of the second option, the wave elevation has to be calculated by a double summation on the wave numbers.

$$\textit{Option 1 :} \begin{cases} \mathbf{k}_{ij}^f = \mathbf{k}_{ij} \\ \omega_{ij}^f = \sqrt{g\left|\mathbf{k}_{ij}\right| \tan\left(\left|\mathbf{k}_{ij}\right| h\right)} \end{cases} \tag{8}$$

$$\textit{Option 2 :}\quad \begin{cases} \omega_n^f = \omega_n \\ \sqrt{\left|\mathbf{k}_n^f\right| \tan\left(\left|\mathbf{k}_n^f\right| h\right)} = \omega_n^f \end{cases} \tag{9}$$

$$\begin{cases} \mathbf{k}_n^f = \left(\left|\mathbf{k}_n^f\right| \cos\theta_{ij}^{(n)} \;,\; \left|\mathbf{k}_n^f\right| \sin\theta_{ij}^{(n)} \right) \\ \theta_{ij}^{(n)} = \arctan\left(k_{y_j}^{(n)} \Big/ k_{x_i}^{(n)} \right) \quad \text{where} \quad \mathbf{k}_{ij}^{(n)} = \mathbf{k}_{ij}\left(\underline{A_{ijn}} \,,\, \omega_n \right) \end{cases} \tag{10}$$

The choice of the complex amplitudes which shall be associated to the derived linear wave components is much more delicate. One has to keep in mind that:

- The filtered frequencies and wave numbers selected by one or the other option mentioned above are different from the ones of the original wave components.
- The energy of the original wave components is spread over all the frequencies and wave numbers of the Fourier space.
- The latter point also implies that energy is allocated to 3D Fourier components which travel in the opposite direction of the original waves. This is shown on Figure 5 which represents amplitude spectrum of the synthetic linear wave field in the 2D Fourier wave number space (ie for each Fourier wave number, the 3D Fourier amplitudes have been summed over the Fourier frequencies). Although the synthetic linear waves are travelling in positive x direction (see (6)), energy is assigned to negative k_x.

Regardless of the fact that is impossible to find the original wave components back, the question of determining the right amount of energy to be allocated to each derived linear wave component is a very delicate issue (see [13]).

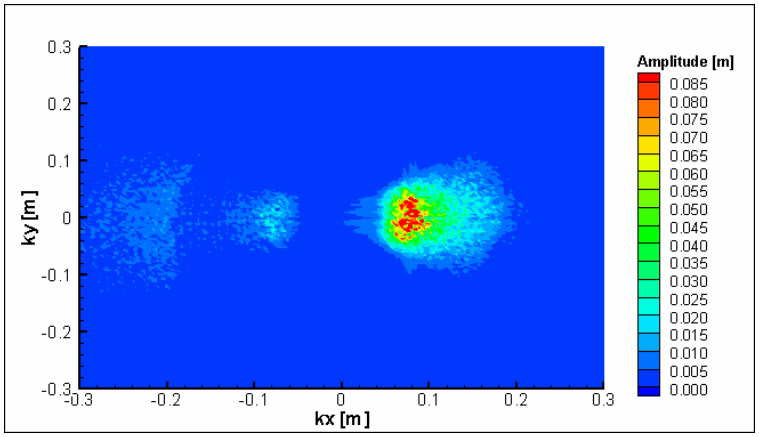

Figure 5 : Amplitude spectrum of the synthetic linear wave field in the 2D Fourier wave number space.

Different methods have been tested to find a proper estimation of the observed wave field with linear wave components derived from the results of a 3DFFT applied to these wave observations. They are extensively detailed in [13] and will not be recalled here. We will only describe the method which was found to give the best results. It is referred to as Method 2c in papers [13] and [7] and consists in:

- Considering Option 1 described in (8) for the choice of the wave numbers and frequencies of the derived linear wave components: the wave numbers are the 2D Fourier wave numbers and the angular frequencies are obtained from these wave numbers via the LDR.
- Regarding the choice of the complex wave amplitude to be assign to a component of wave number $\mathbf{k}_{ij}^f = \mathbf{k}_{ij}$, we consider the sum of the complex amplitudes of the 3D Fourier components associated to the wave number $\mathbf{k}_{ij}$. The energy carried by the 3D Fourier

wave components travelling in the opposite direction to the wave field is also taken into account. Since this energy was initially carried by wave components propagating in the direction of the wave field, we assign it to the direction of wave field (therefore, the minus sign in the first part of expression (11)).

- The estimated surface elevation $\hat{\eta}(\mathbf{x},t)$ is then obtained by applying (11).

$$\hat{\eta}(\mathbf{x},t) = \sum_{i=1}^{N_x/2+1} \sum_{j=1}^{N_y} \left(\sum_{n=1}^{N_t/2+1} \underline{A_{ijn}} \exp\left[-i\,\omega_{ij} t\right] + \sum_{n=N_t/2+2}^{N_t} \underline{A_{ijn}} \exp\left[-i\,\omega_{ij} t\right] \right) \exp\left[i\,\mathbf{k}_{ij} \cdot \mathbf{x}\right] + \text{conj} \tag{11}$$

To optimize the calculation costs, the surface elevation at a given time step of the observation domain is calculated by an inverse 2DFFT in space of the time dependant complex amplitudes $\underline{A_{ij}^{obs}(t)}$ defined by (12). Since the 2DFFT is periodic in space, the surface elevation is identical in any other domain of same size $L_x \times L_y$ being distant from the observation zone by an integer times of its length.

$$\underline{A_{ij}^{obs}(t)} = \sum_{n=1}^{N_t/2+1} \underline{A_{ijn}} \exp\left[-i\,\omega_{ij} t\right] + \sum_{n=N_t/2+2}^{N_t} \underline{A_{ijn}} \exp\left[-i\,\omega_{ij} t\right] \tag{12}$$

Note

To enable noise filtering in case this method would be used on real data, a first broad filter (a Gaussian filter for example) can be applied around the dispersion relation, as it is currently done in Radar IP, to distinguish measurement noise from waves. The wave field is then estimated as follows, where f_{ijn} is a board filter around the linear dispersion relation. The counterpart is of course that wave information will be lost.

$$\hat{\eta}(\mathbf{x},t) = \sum_{i=1}^{Nx/2+1} \sum_{j=1}^{Ny} \left(\sum_{n=1}^{Nt/2+1} \underline{A_{ijn}} \exp\left[-i\,\omega_n t\right] f_{ijn} + \sum_{n=Nt/2+2}^{Nt} \underline{A_{ijn}} \exp\left[-i\,\omega_n t\right] f_{ijn} \right) \exp\left[i\,\mathbf{k}_{ij} \cdot \mathbf{x}\right] + conj \tag{13}$$

III.3 Reconstruction and prediction results

In this section, we compare the *reconstruction* and the *prediction* results obtained by the proposed approach III.2 to the results we would obtain by simply using a comparable output of a Radar IP analysis, ie a periodic wave field in both space and time domains. We recall that the *reconstruction* is the estimation of the wave field within the spatio-temporal observation zone of size $L_x \times L_y \times T$, whereas the *prediction* is the estimation of the wave field which has propagated further in time (ie $t > T$). In this study, the area in space in which prediction calculation are made is of same size as the observation zone and is attached to it along the x-axis (see Figure 4).

As detailed in [7], an accurate prediction of the waves can only be obtained in a specific domain in time and space which is called the *prediction zone.* This specific area depends on sea state properties and the observation zone size and is estimated theoretically from these data. The following prediction results will thus be compared to the theoretical predictability of the measured wave field. (In the observation zone, the theoretical calculation error is zero since all the wave components are supposed to be known).

In the proposed approach, the wave field is calculated by (13), where f_{ijn} is a Gaussian filter around the LDR defined by equation (15), which would enable noise filtering in a real application. In the Radar IP type approach, the same Gaussian filter is applied to the 3D Fourier

components before applying an inverse 3DFFT to the filtered amplitudes (see (14)). This way, the same amount of wave information is lost in both approaches. In (15), b_ω is the filter bandwidth. It is equal to a fraction of the maximum Fourier frequency.

$$\hat{\eta}(\mathbf{x},t) = \sum_{i=1}^{Nx/2+1}\sum_{j=1}^{Ny}\left(\sum_{n=1}^{Nt/2+1}\underline{A_{ijn}}\exp[i\,\omega_n t]f_{ijn} \quad + \sum_{n=Nt/2+2}^{Nt}\underline{A_{ijn}}\exp[-i\,\omega_n t]f_{ijn}\right)\exp[i\,\mathbf{k}_{ij}\cdot\mathbf{x}] + conj \tag{14}$$

$$\begin{cases} f_{ijn} = \exp\left[-0.25\left(\dfrac{\omega_n - \omega(\mathbf{k}_{ij})}{b_\omega}\right)^2\right] \\ b_\omega = \omega_{Nt/2+1}/4 \end{cases} \tag{15}$$

The results presented in the figures bellow have been averaged on 500 realizations. The figures show maps of the error between synthetic and estimated wave fields, as well as theoretical errors (see [7]). Calculation errors are obtained by expression (16) where N_R is the number of realizations (N_R=500). The error maps are shown in the observation zone at 3 different times (see Figure 6 for t=0s, $t=T/2$ and $t=T-\Delta T$), and in the investigated prediction zone at 3 different times also (see Figure 7, for $t=T$, $t=2T$ and $t=t_{\max}$). $t_{\max}$ is the maximum predictable time according to the predictability theory. White lines on Figure 7 represent the limits of the area where the theoretical prediction error is zero.

$$\varepsilon rr(\mathbf{x},t) = \frac{1}{N_R}\sum_{s=1}^{N_R}\frac{\left|\eta^s(\mathbf{x},t) - \hat{\eta}^s(\mathbf{x},t)\right|}{H_s/2} \tag{16}$$

Reconstruction results

Figure 6 shows that the wave field is better reconstructed with the Radar type IP approach. As a matter of fact, it just consists in applying a 3DFFT on the observed wave maps, filtering the 3D Fourier amplitudes by means of a broad filter around the LDR (ie keeping most of the initial wave information), and finally applying an inverse 3DFFT on the filtered amplitudes. Therefore, the reconstructed wave field is almost equivalent to the initial synthetic one, except for a small loss of wave information due to the filtering (but since the filter is relatively broad, only 3D wave components with non significative energy are filtered out).

When manipulating the 3D Fourier wave components following the approach suggested in III.2, the reconstruction error is increasing in time. As a matter of fact, from the 2nd time step $t=\Delta t$ of the measurement duration there is a high error zone entering the observation zone which propagates further in time in the positive x-axis. The explanation of this phenomenon is note quite clear yet, but it is related to the fact that the same linear wave components are used to describe the surface elevation in the entire observation area in space, although in reality, waves enter and leave this area when time increases.

Prediction results

On the other hand, when considering Figure 7, it is obvious that the Radar type IP method is not able to predict accurately the wave field. As a matter of fact, we remind that when using the Radar IP approach the surface elevation in $[L_x,2L_x]\times[0,L_y]\times[T,2T]$ (or at further times $[L_x,2L_x]\times[0,L_y]\times[2T,3T]$) is exactly the same than the reconstructed wave field in the observation domain $[0,L_x]\times[0,L_y]\times[0,T]$ due to the periodicity of the 3DFFT. This is not the case for the synthetic wave field. The prediction results obtained with this approach are thus very poor.

When applying the proposed manipulation method however, the derived linear wave components propagate in time, and periodicity in time is avoided. The prediction results are thus much more accurate. Besides, the prediction error obtained with this method shows very good agreement with the predictability theory.

IV. CONCLUSION

In this paper, we present results on ongoing research projects about deterministic prediction of short-crested waves, based on X-Band Radar measurements. In a first approach we consider perfect wave observations instead of Radar observations. These wave observations are created by means of a linear wave model. The prediction is based on a 3D Fourier analysis of observations, as commonly applied in Radar imaging systems. The purpose of the presented work is to investigate the possibilities of determining a proper initialization for a wave propagation model from the results of a 3DFFT applied to a stack of wave images.

We show that the 3D Fourier wave components obtained by applying a 3DFFT to a sequence of wave images cannot be used directly to initialize a wave propagation model. As a matter of fact, spectral leakage occurs in both space and time domains. Even when considering linear wave data, wave components are produced whose wave number and frequencies do not satisfy the LDR. These components cannot be used to initialize wave propagation. Therefore we propose a method to manipulate these 3D Fourier wave components to derive linear wave components that can be used to initialize a propagation model. This method considers the LDR as a filter and aims to lose the least wave information as possible. The proposed method shows very good prediction results, which are in good agreement the predictability theory.

However, these results concern perfect observation data. Future research will focus on more realistic wave observations including noise for example. Possible alternatives to the 3D FFT approach will be investigated.

V. ACKNOWLEDGEMENTS

This research has been carried out within the “PROMISED Operations” project (PRediction Of wave induced Motions and forces In Ship, offshorE and Dredging Operations), funded by “Agency NL”, a department of the Dutch Ministery of Economic Affairs, Agriculture and Innovation and co-funded by TU Delft, University of Twente, MARIN (MAritime Research Institute Netherlands), Ocean Waves GMBH, Allseas, Heerema Marine Contractors and IHC.

Theoretical reconstruction errors

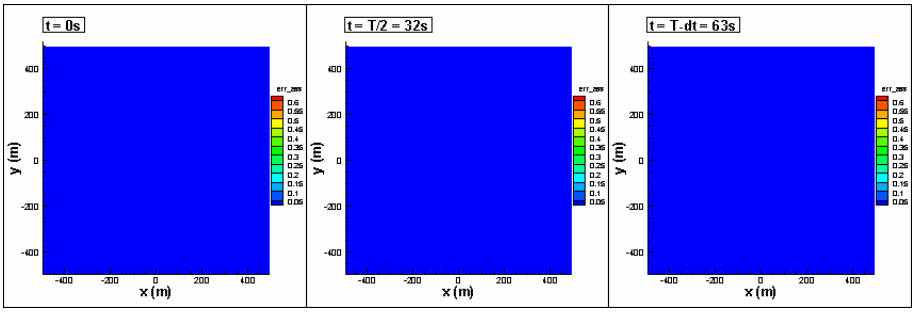

Reconstruction errors obtained with the Radar IP type approach

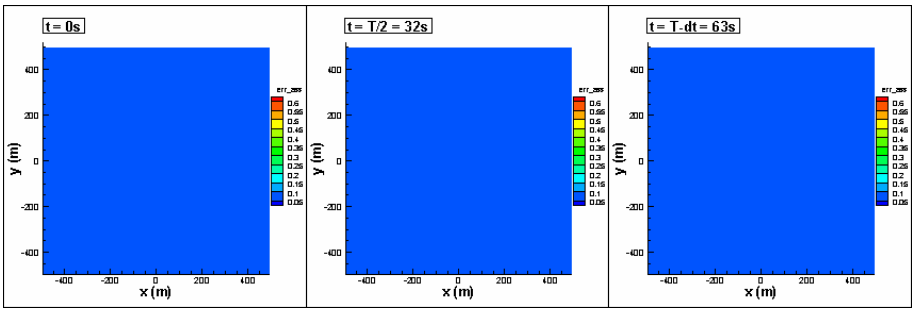

Reconstruction errors obtained with the proposed approach

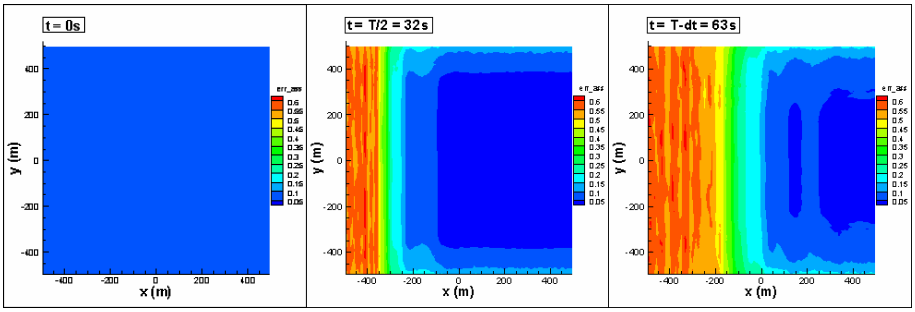

Figure 6 : Reconstruction error maps.

Theoretical prediction errors

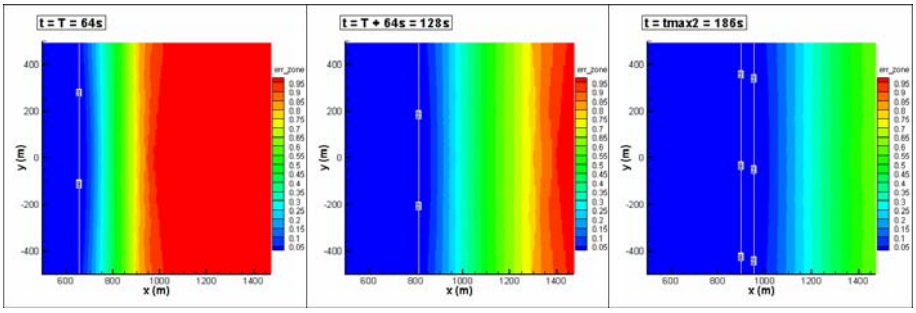

Prediction errors obtained with the Radar IP type approach

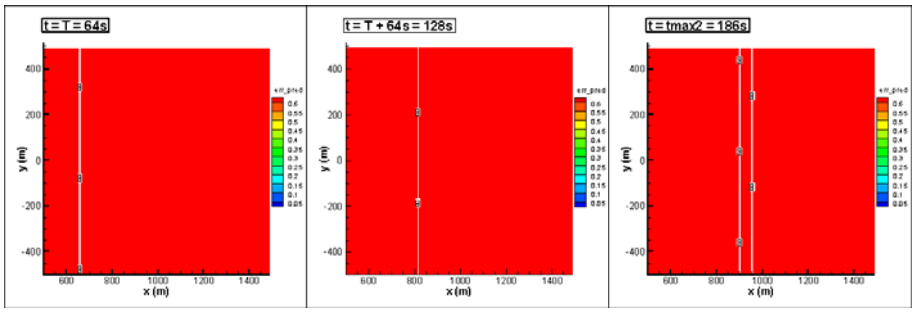

Prediction errors obtained with the proposed approach

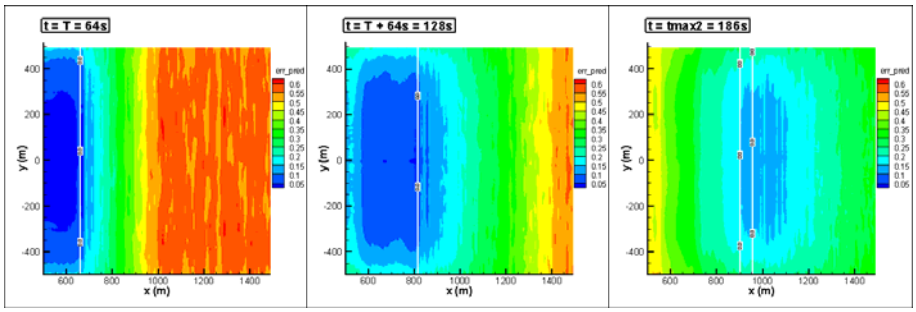

Figure 7 : Prediction error maps.

REFERENCES

[1] L. Abusedra and M.R. Belmont. Prediction diagrams for deterministic sea wave prediction and the introduction of the data extension prediction method. *Intern. Shipbuilding Progress*, 58(1):59–81, 2011.

[2] M.R. Belmont. Application of non-uniform to uniform data mapping to: Shallow angle lidar with the introduction of independent variable techniques. *Signal Processing*, 87(10):2461 – 2472, 2007. Special Section: Total Least Squares and Errors-in-Variables Modeling.

[3] E. Blondel. *Reconstruction et prévision déterministe d'états de mer à partir de données mesurées*. PhD thesis, Ecole Centrale Nantes, 2009.

[4] E. Blondel, F. Bonnefoy, and P. Ferrant. Deterministic non-linear wave prediction using probe data. *Ocean Engineering*, 37(10):913 – 926, 2010.

[5] E. Blondel, F. Bonnefoy, and P. Ferrant. Experimental validation of deterministic non-linear wave prediction schemes in 2d. In *Proceedings of the 20th (2010) International Offshore and Polar Engineering Conference (ISOPE2010), Beijing, China*, 2010.

[6] E. Blondel, F. Bonnefoy, and P. Ferrant. Experimental validation of non-linear deterministic prediction schemes for long-crested waves. *Ocean Engineering, in press*, 2012.

[7] E. Blondel-Couprie and P. Naaijen. Reconstruction and prediction of short-crested seas based on the application of a 3d-fft on synthetic waves. part 2: Prediction. In *Proceedings of the 31th International Conference on Ocean, Offshore and Arctic Engineering (OMAE2012), 01/06 July 2012, Rio (Brasil)*, 2012.

[8] G.F. Clauss, S. Kosleck, and D. Testa. Critical situations of vessel operations in short crested seas – forecast and decision support system –. In *Proceedings of the ASME 2009 28th International Conference on Ocean, Offshore and Arctic Engineering (OMAE2009)*, 2009.

[9] D.G. Dommermuth and D.K. P. Yue. A high-order spectral method for the study of nonlinear gravity waves. *Journal of Fluid Mechanics*, 184:267–288, 1987.

[10] S. Grilli, C-A. Guérin, and B. Goldstein. Ocean wave reconstruction algorithms based on spatio-temporal data acquired by a flash lidar camera. In *Proceedings of the 21st International Offshore (Ocean) and Polar Engineering (ISOPE2011) Conference, Hawai*, 2011.

[11] K. G. Hessner, J. C. Nieto-Borge, and P. S.y Bell. Nautical radar measurements in europe: Applications of wamos ii as a sensor for sea state, current and bathymetry. In Vittorio Barale and Martin Gade, editors, *Remote Sensing of the European Seas*, pages 435–446. Springer Netherlands, 2008. 10.1007/978-1-4020-6772-3_33.

[12] E.L. Morris, H.K. Zienkiewicz, and M.R. Belmont. Short-term forecasting of the sea-state. *Intern. Shipbuilding Progress*, 45(444):383–400, 1998.

[13] P. Naaijen and E. Blondel-Couprie. Reconstruction and prediction of short-crested seas based on the application of a 3d-fft on synthetic waves. part 1: Reconstruction methods. In *Proceedings of the 31th International Conference on Ocean, Offshore and Arctic Engineering (OMAE2012), 01/06 July 2012, Rio (Brasil)*, 2012.

[14] P. Naaijen and R.H.M. Huijsmans. Real time wave forecasting for real time ship motion predictions. In *Proceedings of the ASME 2008 27th International Conference on Ocean, Offshore and Arctic Engineering (OMAE2008)*, 2008.

[15] P. Naaijen and R.H.M. Huijsmans. Real time prediction of second order wave drift forces for wave force feed forward in dp. In *Proceedings of the ASME 2010 29th International Conference on Ocean, Offshore and Arctic Engineering (OMAE2010)*, 2010.

[16] P. Naaijen, R.R.T. van Dijk, R.H.M. Huijsmans, and A.A. El-Mouhandiz. Real time estimation of ship motions in short crested seas. In *Proceedings of the ASME 2009 28th International Conference on Ocean, Offshore and Arctic Engineering (OMAE2009)*, 2009.

[17] J.C. Nieto Borge, C. José, G.R. Rodriguez, K. Hessner, and P.I. Gonzalez. Inversion of marine radar images for surface wave analysis. *Journal of Atmospheric and Oceanic Technology*, 21(8):1291–1300, 2004.

[18] G. Wu. *Direct Simulation and Deterministic Prediction of Large-scale Nonlinear Ocean Wave-field*. PhD thesis, Massachusetts Institute Of Technology, 2004.

[19] I. R. Young, Rosenthal W., and Ziemer F. A three-dimensional analysis of marine radar images for the determination. *Journal of Geophys. Res. Part C, Oceans and atmospheres*, 90(1):1049–1059, 1985.

[20] J. Zhang, J. Yang, J. Wen, I. Prislin, and K. Hong. Deterministic wave model for short-crested ocean waves: Part i. theory and numerical scheme. *Applied Ocean Research*, 21(4):167–188, 1999.